Available online at www.sciencedirect.com
SCIENCE DIRECT®
Journal of Solid State Chemistry 177 (2004) 4475–4481
JOURNAL OF SOLID STATE CHEMISTRY
www.elsevier.com/locate/jssc

Synthesis and characterization of a NaSICON series with general formula $Na_{2.8}Zr_{2-y}Si_{1.8-4y}P_{1.2+4y}O_{12}$ ($0 \leqslant y \leqslant 0.45$)

A. Essoumhi[a], C. Favotto[a], M. Mansori[b], P. Satre[a,*]

[a] *Laboratoire de Physico-chimie du Matériau et du Milieu Marin, Faculté des Sciences et Techniques, Université de Toulon et du Var, 83957 La Garde Cedex, France*

[b] *Laboratoire de Chimie des Matériaux et de l'environnement, Faculté des Sciences et Techniques, Université Cadi Ayyad, B.P. 549, 40000 Marrakech-Maroc, France*

Received 23 July 2004; received in revised form 17 September 2004; accepted 20 September 2004
Available online 11 November 2004

Abstract

In this work, we present the synthesis and the characterization of ionic conducting ceramics of NaSICON-type (Natrium super ionic conductor). The properties of this ceramic make it suitable for use in electrochemical devices. These solid electrolytes can be used as sensors for application in the manufacturing of potentiometric gas sensors, for the detection of pollutant emissions and for environment control. The family of NaSICON that we studied has as a general formula $Na_{2.8}Zr_{2-y}Si_{1.8-4y}P_{1.2+4y}O_{12}$ with $0 \leqslant y \leqslant 0.45$. The various compositions were synthesized by produced using the sol–gel method. The electric properties of these compositions were carried out by impedance spectroscopy. The results highlight the good conductivity of the $Na_{2.8}Zr_{1.775}Si_{0.9}P_{2.1}O_{12}$ composition.

Keywords: Sol–gel method; NaSICON; Electrical conductivity; Impedance spectroscopy

1. Introduction

Since the work of Hong and Goodenough [1,2], many studies have been carried out on a conductive membrane using sodium ions, NaSICON (acronym for Natrium super ionic conductor), for its applications in the fields of energy. The structure of the NaSICON-type ($Na_{1+x}Zr_2Si_xP_{3-x}O_{12}$, with $0<x<3$) has a rhombohedral symmetry, except in the interval $1.8<x<2.2$, where a small distortion of monoclinic symmetry takes place. Compounds in this composition range have a structure made by a three-dimensional framework of SiO_4 and PO_4 tetrahedra corners shared with MO_6 octahedra, in which Na ions occupy the interstices [1,3]. Therefore, these compounds show a very high Na^+ ionic conductivity ($\sigma = 10^{-3}\,\Omega^{-1}\,cm^{-1}$ at room temperature, for the $x=2$ composition), higher than that of β alumina which has two-dimensional mobility, which make them suitable for use in electrochemical gas sensors [4–6]. Outside the "classical" composition $Na_3Zr_2Si_2PO_{12}$, the structural studies and the electric properties were studied for some Zr deficiency compositions ($Na_{1+x}Zr_{2-x/3}Si_xP_{3-x}O_{12-2x/3}$). In fact, the highest conductivity values were observed in the range $1.6 \leqslant x \leqslant 3.0$ [3,7,8].

The aim of the present work is to study the NaSICON family with general formula $Na_{2.8}Zr_{2-y}Si_{1.8-4y}P_{1.2+4y}O_{12}$ ($0 \leqslant y \leqslant 0.45$) in order to determine the existence of same conductivity areas and to understand the conductive mechanism. The synthesis was made using the sol–gel method; the synthesized precursors were characterized by coupled DTA-TGA. The oxides obtained after pyrolysis of the precursors were identified by X-ray diffraction. Furthermore, the sintered ceramic samples were characterized by electric conductivity. Impedance

*Corresponding author. Fax: +33 4 94 14 24 94.
E-mail address: satre@univ-tln.fr (P. Satre).

0022-4596/$ - see front matter © 2004 Elsevier Inc. All rights reserved.
doi:10.1016/j.jssc.2004.09.026

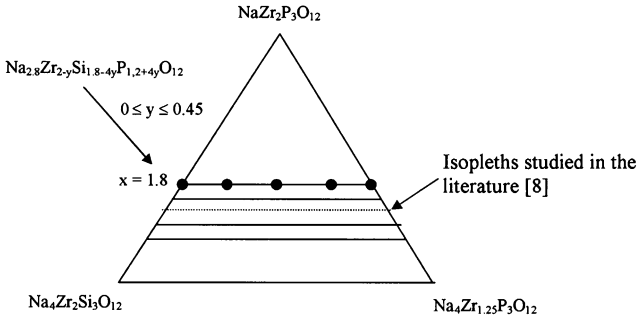

Fig. 1. Compositions diagram.

spectroscopy, used to separate grain from grain boundary impedances, showed that the grain boundary contribution is often the major contribution to the overall impedance [9]. Moreover, this technique enabled us to evaluate the influence of porosity on conductivity.

In the ternary diagram delimited by the compositions $NaZr_2P_3O_{12}$–$Na_4Zr_2Si_3O_{12}$–$Na_4Zr_{1.25}P_3O_{12}$ [10], the studied samples are located on the line with general formula $Na_{2.8}Zr_{2-y}Si_{1.8-4y}P_{1.2+4y}O_{12}$ ($0 \leqslant y \leqslant 0.45$) as shown in Fig. 1. In particular we selected those compositions, which have a constant stoichiometric of Na^+ ions in general formula. The synthesis method of the precursors described in this contribution was used in order to improve the sintering conditions of NaSICON compounds.

2. Experimental

In this study, 5 compositions are explored: $y = 0$; 0.075; 0.225; 0.375 and 0.45, represented by points on Fig. 1. The corresponding samples are respectively noted A ($Na_{2.8}Zr_2Si_{1.8}P_{1.2}O_{12}$), B ($Na_{2.8}Zr_{1.925}Si_{1.5}P_{1.5}O_{12}$), C ($Na_{2.8}Zr_{1.775}Si_{0.9}P_{2.1}O_{12}$), D ($Na_{2.8}Zr_{1.625}Si_{0.3}P_{2.7}O_{12}$) and E ($Na_{2.8}Zr_{1.55}P_3O_{12}$).

Taking into account the difficulty in obtaining pure ceramics of NaSICON by reactions in solid phase, the precursors were synthesized by the sol–gel process in order to obtain the preliminary formation of an amorphous solid (xerogel) [11]. The higher reactivity of these precursors leads more easily to monophasic compositions, without impurities at the grain boundary, and at the same time produces very small grains which are sintered more easily. The synthesis was performed in three stages:

- The first stage consisted in mixing at ambient temperature distilled water, ethanol, tetraethylorthosilicate (TEOS) and nitric acid. The proportions of these compounds were selected in the miscible area of TEOS–ethanol–water phase diagram [12] in order to better homogenize the reactants and try to limit the segregation of zirconia. The pH was adjusted to one after addition of an HNO_3 solution.
- The second stage consisted in simultaneously dissolving stoichiometric quantities of $NaNO_3$ and $ZrO(NO_3)_2$ in distilled water at ambient temperature and adding them to the previous solution while stirring until a clear phase was obtained.
- Finally, the last stage consisted in quickly adding the di-ammonium-hydrogeno-phosphate solution, a white gelatinous precipitate appeared. The mixture obtained was dried at 100 °C until the solvent was eliminated and a dehydrated compound was obtained.

Many works [13,14] show that the procedures of the powder preparation and the later heat treatments strongly affect the ceramic properties containing NaSICON. All the studied samples were submitted to the same calcinations and sintering treatments. The precursors were calcined at 1000 °C for 3 h under air. The powders were uniaxially pressed (120 MPa) into pellets of 13 mm in diameter and sintered under air at 1050 °C for 70 h. The heating-cooling rates were equal to 5 °C min^{-1}. The final density of the ceramics was obtained from their geometrical dimensions and their masses. The diameters of the NaSICON samples were 13 mm and the thicknesses were in the range of 1–1.5 mm.

For all the studied compositions, the optimum conditions for calcination of the precursors were determined by DTA-TGA coupled (Setaram TGA92) between room temperature and 1100 °C, and the heating rate was 10 °C min^{-1}. After pyrolysis, the calcined powders were characterized by X-ray diffraction at room temperature (Siemens D5000, $\lambda_{Cu} = 1.5406$ Å).

The electrical properties of ceramics were determined by ac impedance spectroscopy measurements (Hewlett-Packard 4194A) between 25 and 110 °C under air, in the frequency range 100–4×10^7 Hz. An applied voltage was fixed at 100 mV. The sample was allowed to equilibrate for 2 h before measurements could be obtained of the reproducible impedance spectra. The measurement electrodes were made of platinum deposited by cathodic sputtering at room temperature (Plassys MP300).

3. Results and discussions

3.1. Coupled DTA-TGA

The five thermograms obtained are similar and present three successive mass losses associated with thermal phenomena (endothermic or exothermic). Fig. 2 presents the results obtained for the composition $y = 0.225$:

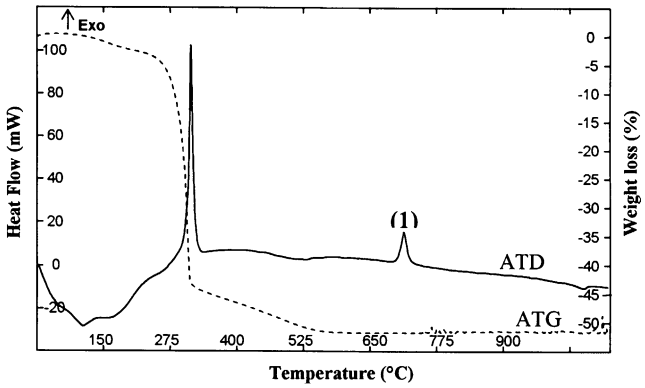

Fig. 2. Curves DTA-TGA of the composition $y=0.225$.

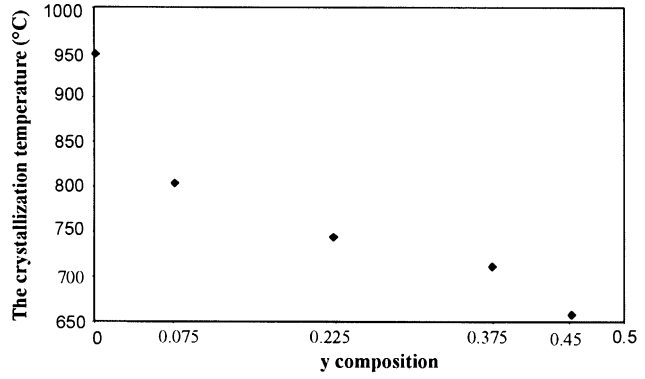

Fig. 3. The crystallization temperature evolution according to the NaSICON composition.

- A first loss occurs between 40 and 230 °C: the endothermic phenomenon observed corresponds to the loss of water and residual solvent.
- A second loss occurs between 230 and 335 °C: the exothermic peak was attributed to the removal of a residual organic group.
- A third loss occurs between 335 and 575 °C: the departure of the water and solvent trapped in closed pores [15] (endothermic phenomenon).

The exothermic peak at 730 °C, note accompanied by weight losses represents the crystallization phase of NaSICON.

Fig. 3 shows the crystallization temperature evolution (peak exothermic noted (1)) according to the NaSICON composition.

For sample A ($y=0$), the crystallization temperature value of the precursor is in agreement with those obtained in the literature for zirconium non-deficiency compositions elaborated using the sol–gel method [16–18]. For solid solutions of general formula $Na_3Zr_{2-x/4}Si_{2-x}P_{1+x}O_{12}$ (with $0<x<2$), the crystallization temperature decreased [9,19]. The stage of crystallization occurs between 650 and 750 °C (Fig. 3). It is important to note that any considerable variation of the crystallization temperature for the NaSICON phase with the zirconium concentration ($\Delta T=300$ °C between $y=0$ and $y=0.45$) has not been described, to our knowledge, in the literature.

3.2. X-ray diffraction at room temperature

The different oxides obtained after pyrolysis of the precursors were analyzed by X-ray diffraction. The X-diagrams obtained at room temperature for the compositions $y=0$, 0.075 and 0.225 showed only the presence of the NaSICON single-phase. We presented in Fig. 4 one example of three representative samples, corresponding to the composition $y=0.225$.

The analysis shows that, for y values in range 0 and 0.225, the dominant phase after pyrolysis is NaSICON without any detected trace of ZrO_2. No other phase such as SiO_2, $ZrSiO_4$, Na_3PO_{12}, Na_2SiO_3 or Na_2ZrO_3 could be detected in these samples. The low full widths at half maximum (FWHM) of the diffraction peaks indicate that the crystallization of the NaSICON phase is effectively under the experimental conditions, in agreement with the results of thermal analysis (Fig. 3). The results obtained for these three compositions suggest that a decrease in the zirconium concentration does not modify the stability of the NaSICON phase [7,20]. In the absence of any ZrO_2 trace (Fig. 4), we can suggest that no volatilization phenomenon of Na and P occurred up to 1000 °C [21].

For the weakest zirconium concentrations ($y=0.375$ and 0.45), the stage of calcinations at 1000 °C involves the appearance of the additional phases, which were identified as ZrO_2 and Na_3PO_4 (Fig. 5). The presence of ZrO_2 seems to correspond to a phase separation of NaSICON at high temperature. This result is surprising because the thermal decomposition of NaSICON is generally observed at higher temperatures above 1000 °C [17–18,22]. However, Yang and Liu [23] detected the presence of ZrO_2 after a thermal treatment at 780 °C during 1 h of an $Na_3Zr_2Si_2PO_{12}$ powder synthesized by the sol–gel process. The results of this

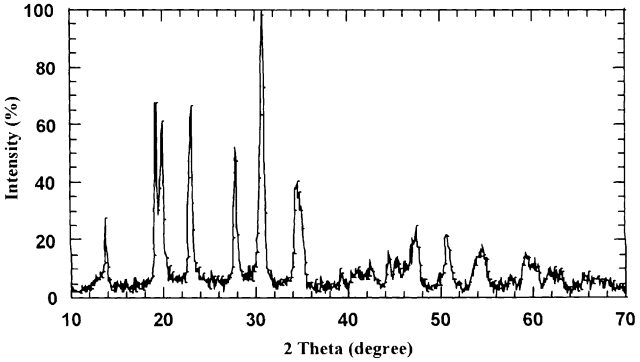

Fig. 4. X-ray diffraction diagram for the composition $y=0.225$.

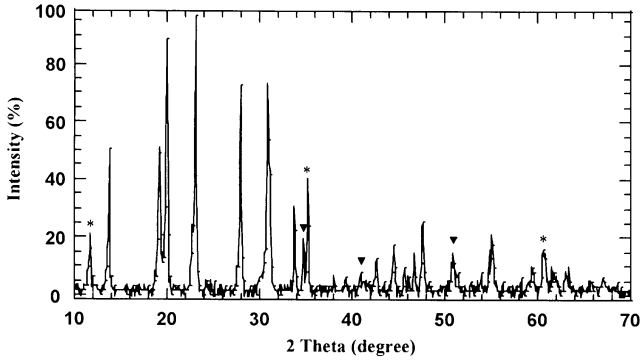

Fig. 5. X-ray diffraction diagram for the composition $y=0.45$. ▼: ZrO_2;*: Na_3PO_4.

study indicate that a heat treatment carried out at temperatures of 200 °C higher than the crystallization temperature of the NaSICON phase led to the thermal decomposition of this compound.

3.3. Sintering

As the temperature of the sintering isothermal stage corresponds to the calcination temperature of the precursors, no notable modification of the chemical composition was expected after sintering. The relative density of the samples had been measured pycnometrically on the samples used for conductivity. For the samples A–C ($y<0.3$) it was equal to 94% of the theoretical density. For the samples D and E, the relative density is, respectively, 90% and 87% of the theoretical value. In disagreement with certain results of the literature [9,22], the zirconium content does not seem to have a notable incidence on the densification of the studied compounds when $y<0.3$. Indeed, Bohnke et al. [9] noted that a final density was greater for $Na_3Zr_{2-x/4}Si_{2-x}P_{1+x}O_{12}$ of about 30% when x increases up to 1.333. For the ceramics of the same general formula, Traversa et al. [20] showed that the process of sintering proceeds in two stages. In the case of $Na_3Zr_2Si_2PO_{12}$, only one shrinkage phenomenon was observed. Indeed, the contribution of the second stage of sintering, occurring at temperatures in the range 950 and 1050 °C, is more significant as the phosphorus content is high. This process, described at the highest reached temperatures, was attributed to a process of liquid phase sintering [13,24,25].

The results of this study are not in contradiction with the literature ([14] stress that the observation of a vitreous phase necessitates sintering durations greater than 2 h). In our works the duration of sintering is 70 h. However, an increase in the y value up to 0.45 can promote the liquid phase formation for temperatures of about 1000 °C [20]. For example, the densification of $Na_3Zr_{1.667}Si_{0.667}P_{2.333}O_{12}$ compound is mainly due to a sintering process in liquid phase and the maximum shrinkage is observed at nearly 1050 °C. The appearance of a liquid phase may induce the segregation of zirconia crystals by dissolution—precipitation process [9] or the doping agents during high heating treatments [26]. In addition, the presence of an important proportion of a liquid phase does not allow relative densities higher than 92% of the theoretical density [20,27]. Therefore, the description of ZrO_2 and Na_3PO_4 for y values higher than 0.3 and the diminution in the relative density for the samples D and E suggest the existence of a liquid phase for temperatures close to 1000 °C.

3.4. Impedance spectroscopy

One of the interests of the impedance spectroscopy resides in its capacity to separate the electric contributions from the matrix grains of NaSICON and the microstructural defects (grain boundary, second phases) [23,28,29]. When $y<0.3$, the geometrical pace of the impedance experimental diagrams is similar (Fig. 6). The contribution described at the low frequencies characterizes the response of the NaSICON/ electrode interface. In the absence of the second phase, the semicircle observed at average frequency translates the blocking effect of the charge carriers at the grain boundaries. At high frequencies, the impedance diagram, described partially according to the temperature measured, corresponds to the specific response of the matrix grains of NaSICON. For temperatures typically higher than 50 °C, this part is not described in the range of the experimental frequency (Fig. 6). However, the different values between the relaxation frequencies of the respective answers of the grains and the grain boundaries (corresponding to at least the imaginary part of each material contribution) allow a sufficient separation between the two electric contributions. Under these conditions, it is always possible to determine the resistance of the grains of the NaSICON phase by intercepts on the axis of extrapolation realities at high frequencies of the blocking contribution.

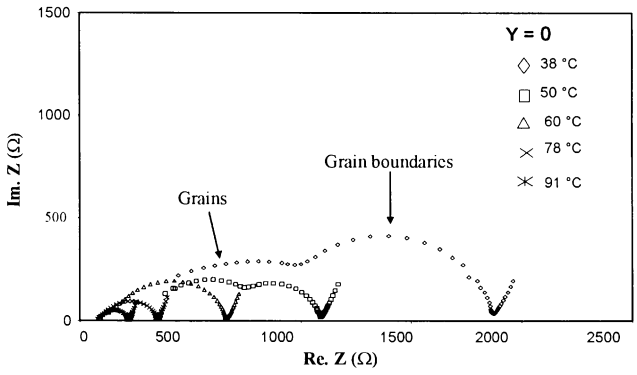

Fig. 6. Impedance diagram for $y=0$ at different temperatures.

Whatever the composition, the clear separation between the response of the grain boundaries and the electrode characteristic allows us to measure without any ambiguity the total resistance of a sample. As Fig. 7 shows, the presence of second phases (for example, insulating like ZrO_2) and of a more significant porosity results in an additional contribution, which strongly interferes with the response of the ceramic grains [30,31]. Under these conditions, respective resistances of the various material contributions could not be given with sufficient precision. The electric behavior of the samples D and E will be described, in the continuation, only starting from total conductivity.

The effect of blocking typically represents 40% of the total resistance of material for the samples A and B (Fig. 6). In the case of the sample C ($y=0.225$), 70% of the total resistive contribution of material is due to the blocking resistance. Taking into account the dominating influence of the microstructure on the amplitude of the blocking effect of the charge carriers [9,14], all comparison with other materials must be carried out with caution.

The evolution of total conductivity (σ_{tot}) in Arrhenius coordinates is represented in Fig. 8. The corresponding activation energy (E_a) is given in Table 1. For the studied compositions, E_a varies between 0.24 and 0.37 eV. These values are in agreement with the literature data for NaSICON conductors by sodium ions [9,19,29]. For the composition $y=0$ ($Na_{2.8}Zr_2Si_{1.8}P_{1.2}O_{12}$), which remains similar to the classical NaSICON $Na_3Zr_2Si_2PO_{12}$, the total conductivity and the activation energy are respectively equal to 3.3×10^{-5} S cm^{-1} at 27 °C and 0.37 eV. The E_a value is in agreement with those given for $Na_3Zr_2Si_2PO_{12}$ [14,19,21] but the total conductivity is lower than those generally obtained under the same experimental conditions (to be around 10^{-4} S cm^{-1}). This difference can be explained by a reduction in the concentration in charge carriers. However, it is significant to recall that the microstructure has also a notable influence. For example, Bohnke et al. [9] report a conductivity at 27 °C equal to 8.6×10^{-5} S cm^{-1} in the case of a $Na_3Zr_2Si_2PO_{12}$ sample whose amplitude of the blocking effect of the grain boundaries represents 80% of the total resistance of sintered material.

Table 1
Electric properties of the studied compositions

y	$\sigma_{tot\ (27\,^\circ C)}$ (S cm^{-1})	E_a (eV)	d/d_{th} (%)
0	3.32×10^{-5}	0.37	94
0.075	3.22×10^{-5}	0.24	94
0.225	5.90×10^{-5}	0.29	94
0.375	2.57×10^{-6}	0.27	90
0.450	3.40×10^{-7}	0.31	87

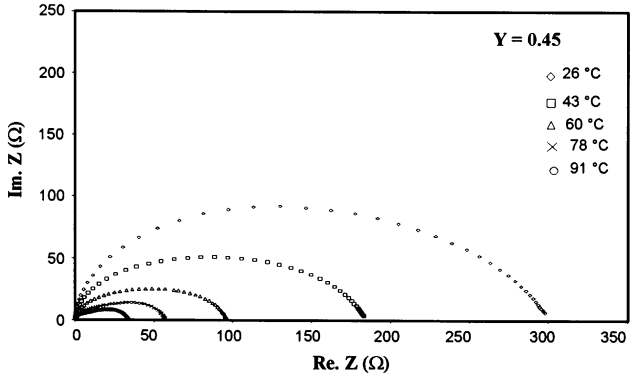

Fig. 7. Impedance diagram for $y=0.450$ at different temperatures.

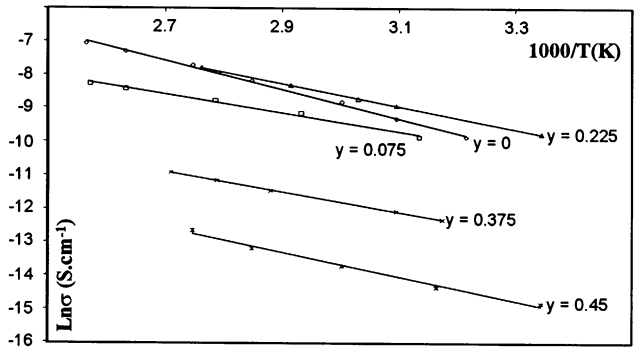

Fig. 8. Arrhenius plots for several studied compositions.

From a general point of view, the reduction in the amount of zirconium is accompanied by a notable degradation of the electric properties of studied materials only for y values higher than 0.3 (Fig. 8) in general formula $Na_{2.8}Zr_{2-y}Si_{1.8-4y}P_{1.2+4y}O_{12}$, in agreement with the results of Bohnke et al. [9]. For example, the total conductivity at 27 °C is ten times less for sample E than for sample A (Table 1). In the absence of any precise conductivity determination of the ceramic grains when $y>0.3$, it is not possible, at this stage of the study, to quantify the influence of the microstructure compared to the possible reduction in the concentration of charge carriers on the total variation σ_{tot}. For samples D and E, the strong conductivity reduction can be mainly linked to an increase in porosity and the presence of second insulating phase ZrO_2 [19].

For temperatures typically lower than 100 °C, the σ_{tot} variations are lower than a factor of 2 when $y<0.3$. Bohnke et al. [9] showed that the total conductivity of $Na_3Zr_{2-x/4}Si_{2-x}P_{1+x}O_{12}$ compounds decreases by a factor 4 when x varies between 0 and 1. In the same way, the total conductivity of dense ceramics (95% of the theoretical density) decreases by a factor of more than 10 between the samples $Na_3Zr_{1.833}Si_{1.333}P_{1.667}O_{12}$ and $Na_3Zr_{1.667}Si_{0.667}P_{2.333}O_{12}$ [19].

In the literature, it is proposed that a modification of the zirconium content modifies the size of the diffusion

channels of the sodium ions and involves a degradation of the electric properties [32,33]. This degradation is accompanied by an increase in the activation energy for the conduction process in the material [9,20]. This is in contradiction with the results of this study. Even for y values higher than 0.3, the activation energy is lower than the ones given for no Zr-deficient ceramics. The reduction in the activation energy indicates a modification of the conduction process. The comparison of the electric properties of dense samples (at least 91% of the theoretical density) of respective formulae $Na_3Zr_2Si_2PO_{12}$ and $Na_{3.2}Zr_{1.3}Si_{2.2}P_{0.8}O_{10.5}$ highlighted a reduction in the activation energy of the total conductivity in the presence of the vitreous phase for the Zr-deficient sample [27]. Fuentes et al. [14] observed the same behavior for an NaSICON type compound ($Na_3Zr_{1.88}Si_2Y_{0.12}O_{12}$). An increase in the volumic fraction of the vitreous phase to the grain boundaries is accompanied by a reduction in the activation energy from 0.39 to 0.26 eV [14]. Moreover, the total conductivity of these ceramics decreases qualitatively with the content of vitreous phase. These observations are in agreement with the results of this study. Under these conditions, the variations of the electric properties of studied materials militate in favor of the presence of a liquid phase at high temperature.

The comparison of the grain and grain boundaries conductivities for compositions such as $y<0.3$ (Table 2) is also in favor of this assumption. Indeed, in absence of any modification of the chemical nature of the grain boundaries in these dense samples, the conduction properties in the grain volume and on the level of the grains must vary in a similar way. Thus, the conductivity values of the grain σ_g and the grain boundaries σ_{jg} decrease respectively by a factor of 1.5 and a factor of 2 at 50 °C when y varies between 0 and 0.075. On the other hand, when y increases from 0.075 to 0.225, σ_g increases by a factor of 4.5 whereas σ_{jg} is multiplied only by a factor of 1.5. This variation type was already observed for nanometric anion conductors (ZrO_2–M_2O_3) whose blocking effect due to the grain boundaries is prevalent [34]. It was interpreted in terms of the M^{3+} ions segregation to the grain boundaries. Under these conditions, the weak increase in σ_{jg}, compared to σ_g, could be connected to a Zr^{4+} ion segregation of the grain boundaries due to the presence of a vitreous phase [9] without notable precipitation of ZrO_2. An increase in the y value leads simultaneously to a more important variation of the zirconium concentration in the grain volume due to a vitreous phase and to ZrO_2 precipitation. The total conductivity of material then decreases notably.

Table 2
Grain (σ_g) and grain boundaries (σ_{jg}) conductivity

y	$y=0$	$y=0.075$	$y=0.225$
T (°C)	50	50	50
σ_g (S cm^{-1})	1.39×10^{-4}	9×10^{-5}	4.06×10^{-4}
σ_{jg} (S cm^{-1})	2.52×10^{-4}	1.24×10^{-4}	1.87×10^{-4}
σ_{tot} (S cm^{-1})	8.96×10^{-5}	5.21×10^{-5}	1.28×10^{-4}

One of the significant parameters of the electric properties optimization for the studied compounds is the grain conductivity σ_g [9,32]. As it was observed for the total conductivity σ_{tot}, the σ_g value is a maximum for the $Na_{2.8}Zr_{1.775}Si_{0.9}P_{2.1}O_{12}$ sample. In spite of an increase in the amplitude of the blocking effect due to the microstructural defects for $y=0.225$, the NaSICON-type compounds showing the best conductivities are the ones whose intragranular conductivities are the highest at temperatures lower than 100 °C.

4. Conclusion

The sol–gel method used allows us to synthesize the precursors of NaSICON-type compounds with general formula $Na_{2.8}Zr_{2-y}Si_{1.8-y}P_{1.2+y}O_{12}$ at temperatures lower than 1000 °C. The relative densities higher than 90% of the theoretical density were reached for broad compositions range ($0\leqslant y\leqslant0.225$) by classical sintering at 1000 °C. The characterizations undertaken suggest that the sintering process implies a liquid phase at high temperature. For y values higher than 0.3, this liquid phase seems to induce the zirconia segregation of grain boundaries. The total electric conductivity strongly depends on the nature of the microstructural defects (grain boundary and additional phases). The highest total conductivity is obtained for the composition, which shows the strongest intragranular conductivity ($y=0.225$). The conductivity of this composition ($y=0.225$) should be improved increasing the density. These works are in progress and will be published in a future paper.

Acknowledgments

The Chemistry CEZUS Society, Pechiney Group, was partially supplied the necessary raw materials.

References

[1] H.Y.P. Hong, Mater. Res. Bull. 11 (1976) 173–182.
[2] J.B. Goodenough, H.Y.P. Hong, J.A. Kalafas, Mater. Res. Bull. 11 (1976) 203–220.
[3] P. Boilot, P. Colomban, Solid State Ionics 18–19 (1986) 974–980.
[4] N. Miura, S. Yao, Y. Shimizu, N. Yamazoe, Sensors Actuators B 9 (1992) 165–170.
[5] N. Miura, S. Yao, Y. Shimizu, N. Yamazoe, J. Electrochem. Soc. 139 (1992) 1384–1388.
[6] Y. Sadaoka, Y. Sakai, M. Matsumoto, T. Manabe, J. Mater. Sci. 28 (1993) 5783–5792.

[7] U. Von Alpen, M.F. Bell, H.H. Höfer, Solid State Ionics 3–4 (1981) 215–218.
[8] N. Poignet, Elaboration et caractérisation de couches pour microcapteurs électrochimiques à base de NaSICON, Thèse ENSEEG-INP, Grenoble, 1992.
[9] O. Bohnke, S. Ronchetti, D. Mazza, Solid State Ionics 122 (1999) 127.
[10] H. Kohler, H. Schulz, O. Melnikov, Mater. Res. Bull. 18 (1983) 1143.
[11] C. Favotto, L. Tortet, P. Satre, M. Roubin, Sil. Ind. 66 (1–2) (2001) 3–8.
[12] C.J. Brinker, G.W. Scherer, Sol–Gel Science, Academic Press, San Diego, 1990, p. 109.
[13] Ph. Colomban, Solid State Ionics 21 (1986) 97.
[14] R.O. Fuentes, F.M. Figueiredo, F.M.B. Marques, J.I. Franco, Solid State Ionics 140 (2001) 173.
[15] A. El Ghazouli, N. El Moudden, M. Sghyar, M. Rafiq, A. Larbot, L. Cot, Ann. Chim. Sci. Mater. 26 (3) (2001) 41–48.
[16] D.-D. Lee, S.-D. Choi, K.-W. Lee, Sensors Actuators B 24–25 (1995) 607.
[17] T. Kida, Y. Miyachi, K. Shimanoe, N. Yamazoe, Sensors Actuators B 80 (2001) 28.
[18] A. Martucci, S. Sartori, M. Guglielmi, M.L. Di Vona, S. Licoccia, E. Traversa, J. Eur. Ceram. Soc. 22 (2002) 1995.
[19] E. Traversa, H. Aono, Y. Sadaoka, L. Montanaro, Sensors Actuators B 65 (2000) 204.
[20] E. Traversa, L. Montanaro, H. Aono, Y. Sadaoka, J. Electroceram. 5–3 (2000) 261.
[21] A. Ahmad, T.A. Wheat, A.K. Kuriakose, J.D. Canaday, A.G. McDonald, Solid State Ionics 24 (1987) 89.
[22] J. Engell, S. Mortensen, L. Moller, Solid State Ionics 9–10 (1983) 877.
[23] Y. Yang, C.-C. Liu, Sensors Actuators B 62 (2000) 30.
[24] A.K. Kuriakose, T.A. Wheat, A. Ahmad, J. Dirocco, J. Am. Ceram. Soc. 67 (3) (1984) 179.
[25] N. Gasmi, N. Gharbi, H. Zarrhouk, P. Barboux, R. Morineau, J. Livage, J. Sol–gel Sci. Technol. 4 (1995) 231.
[26] F. Krok, Solid State Ionics 24 (1987) 21.
[27] H.-B. Kang, N.-H. Cho, J. Mater. Sci. 34 (1999) 5005.
[28] M.L. Bayard, G.G. Barna, J. Electroanal. Chem. 91 (1978) 201.
[29] W. Bogucz, F. Krok, W. Piszczatowski, Solid State Ionics 119 (1999) 165.
[30] M. Kleitz, L. Dessemond, M.C. Steil, Solid State Ionics 75 (1995) 107.
[31] J. Fleig, J. Maier, J. Electroceram. 1 (1997) 73.
[32] H. Khireddine, P. Fabry, A. Caneiro, B. Bochu, Sensors Actuators B 40 (1997) 223.
[33] D. Tran Qui, J.J. Capponi, M. Gondrand, M. Saib, J.C. Joubert, Solid State Ionics 3–4 (1981) 219.
[34] F. Boulc'h, Thèse, Institut National Poytechnique de Grenoble, 2002.